JOURNAL OF VIROLOGY, Nov. 2009, p. 11540–11549 Vol. 83, No. 22
0022-538X/09/$12.00 doi:10.1128/JVI.02558-08


# Peripheral Immunization Blocks Lethal Actions of Vesicular Stomatitis Virus within the Brain▽

Koray Ozduman, Guido Wollmann, Sebastian A. Ahmadi, and Anthony N. van den Pol*

*Department of Neurosurgery, Yale University School of Medicine, New Haven, Connecticut 06520*

Received 11 December 2008/Accepted 24 August 2009

**Vesicular stomatitis virus (VSV) is the prototype virus for 75 or more negative-strand RNA viruses in the rhabdovirus family. Some of these viruses, including VSV, can cause neurological impairment or death upon brain infection. VSV has shown promise in the prevention and treatment of disease as a vaccine vector and an oncolytic virus, but infection of the brain remains a concern. Three VSV variants, the wild-type-related VSV-G/GFP and two attenuated viruses, VSV-CT1 and VSV-CT9-M51, were compared for neuroinvasiveness and neuromorbidity. In nonimmunized mice, direct VSV-G/GFP injection into the brain invariably resulted in lethal encephalitis; in contrast, partial survival was seen after direct injection of the attenuated VSV strains. In addition, both attenuated VSV strains showed significantly reduced neuroinvasiveness after intranasal inoculation of young postnatal day 16 mice. Of the three tested variants, VSV-CT9-M51 generated the lowest degree of neuropathology. Despite its attenuated state, peripheral inoculations of VSV-CT9-M51 targeted and killed human glioblastoma implanted into the mouse brain. Importantly, we show here that intranasal or intramuscular immunization prevents the lethal effects of subsequent VSV-G/GFP, VSV-CT1, and VSV-CT9-M51 injections into the brain. These results indicate that attenuated recombinant viruses show reduced neurovirulence and that peripheral immunization blocks the lethal actions of all VSVs tested.**

The brain occupies a special niche in viral immunity, and due to a number of mechanisms, viruses in the periphery generally do not enter the brain. However, the same mechanisms that give the brain a special protected status can also impede an immune response against intracerebral infection by viruses. Although many negative-strand RNA viruses can be tolerated peripherally, central nervous system (CNS) infection with vesicular stomatitis virus (VSV), rabies virus, measles virus, influenza virus, and others (14, 24, 28, 30, 34) can be fatal for rodents and for humans. Peripheral immunization does protect the brain from virus infections, but in most studies, it does so by eliminating viruses before they penetrate the blood-brain barrier and enter the brain (4, 25, 29, 38). In contrast, the set of experiments described here address the question of whether peripheral immunization can block the lethal consequences of direct VSV infections within the brain. When injected into the brain, VSV can cause permanent neurological dysfunction in rodents or primates (19, 28) or lethal encephalitis (11, 15). VSV can also enter the brain from the periphery along a cranial nerve, for instance, the olfactory nerve after intranasal administration, and can subsequently spread from the olfactory system to other regions of the brain (24, 36).

Recombinant VSVs have shown promise in two respects: VSV can serve as a robust vaccine vector (26, 27, 16) and as a potent oncolytic virus against a variety of peripheral (1, 3, 10, 33) or CNS (9, 18, 22, 39, 40) tumors. A number of studies have shown the protective effects of peripheral immunization with VSV on peripheral viral infections (12, 13). In contrast, the effect of peripheral immunization on viral infections within the brain has received considerably less attention.

Both as a vaccine vector and as an oncolytic virus, VSV infection of normal brain cells remains a concern. The set of experiments presented here addressed the primary question of whether peripheral immunization can protect the brain from subsequent direct exposure to VSV. A secondary question was whether recombinant VSVs with an attenuated phenotype in culture would also show reduced neurovirulence in the brain.

VSV is an enveloped negative-strand RNA virus, and its 11.2-kb genome encodes five viral proteins (N, P, M, G, and L). VSV is a nonhuman pathogen that can cause a typically self-limiting disease in livestock with flu-like symptoms (20). Limiting factors of VSV for clinical use are its neurotropic properties and the still little understood potential of the brain to fight off a potential infection (5, 6, 15). The brain is largely protected from virus entry through the blood-brain barrier. Mice do not show signs of CNS infection after peripheral VSV application. In contrast, VSV with direct access to the CNS, either experimentally through direct injection or through the intranasal path, can spread through the brain, resulting in encephalitis with high mortality in mice. VSV spread through the brain after intranasal application is age dependent, with mature mice showing little or no spread beyond the olfactory nerve compared to young mice, which succumb to widespread viral infection throughout the brain (19, 36). Peripheral VSV infection triggers fast and effective upregulation of interferon-inducible genes, followed by induction of both the cellular and humoral branches of the systemic immune system.

The extent of VSV pathogenesis in the brain is determined by the replicative efficacy of the virus and the efficiency of the host immune response in curbing the infection. Modification of either of these components can alter the course and extent of CNS damage. In the current work, we used a dual viral muta-

* Corresponding author. Mailing address: Department of Neurosurgery, Yale University School of Medicine, 333 Cedar St., New Haven, CT 06520. Phone: (203) 785-5823. Fax: (203) 737-2159. E-mail: anthony.vandenpol@yale.edu.

▽ Published ahead of print on 2 September 2009.

tion that enhances the host innate cellular immune response (VSV-M51) and truncates the VSV-G cytoplasmic tail from 29 to 9 amino acids (VSV-CT9). Another VSV with a VSV-G truncation to 1 cytoplasmic amino acid (VSV-CT1), resulting in viral attenuation in vitro and in vivo, was also used (23, 31).

Little is known about the extent to which the adaptive immune response can influence VSV within the brain. Here, we show that peripheral VSV immunization prior to intracerebral inoculation prevented lethal encephalitis in adult mice of the strongly attenuated VSV variants, VSV-CT9-M51 and VSV-CT1, as well as a wild-type VSV bearing a green fluorescent protein (GFP) reporter.

## MATERIALS AND METHODS

**Viruses.** Three VSVs were used in the experiments described below. These three viruses have the following genotypes. (i) In VSV-G/GFP, an expression cassette with a GFP sequence fused to VSV-G was inserted between the wild-type G and L genes (8, 36). (ii) In VSV-CT1, the cytoplasmic tail of the G protein was truncated from 29 amino acids to 1 amino acid. (iii) In VSV-CT9-M51, position 51 of the M gene coding for methionine was deleted, and the cytoplasmic tail of VSV-G was reduced from 29 to 9 amino acids. The generation of recombinant VSV strains is described in detail elsewhere (8, 17, 23, 31, 37), and they were kindly provided by J. Rose.

**Animal procedures.** Animal experiments and postoperative care were performed in accordance with the institutional guidelines of the Yale University Animal Care and Use Committee. Normal Swiss-Webster mice and immunodeficient homozygous CB17-SCID (CB17SC-M) mice were obtained from Taconic Inc. The mice were anesthetized by intraperitoneal injection of a combination of ketamine and xylazine (100 and 10 mg/kg of body weight, respectively). Stereotactic intracerebral injections of viruses into the left frontal lobe (1.5 mm lateral and 2 mm rostral to the bregma at 2-mm depth) were performed in 4- to 5-week-old animals. For tumor implants, $3 \times 10^5$ tumor cells were injected bilaterally into the striatum (2 mm lateral and 0.4 mm rostral to the bregma at 3-mm depth). Intranasal virus inoculations were performed under light ketamine-xylazine anesthesia (50 mg/kg and 5 mg/kg, respectively) with a 25-μl inoculum in each nostril.

The animals were immunized through either the intranasal or intramuscular route. The intranasal dose was $2.5 \times 10^7$ PFU VSV-G/GFP given as 25 μl in each naris. The same dose was given 6 weeks later as a boost. Intracranial viral challenge was given 2 weeks after the boost dose.

Intracerebral injections in adult animals were given as a single stereotactic injection of VSV-G/GFP, VSV-CT9-M51, or VSV-CT1 as 200 nl into the left frontal lobe using a 1-μl Hamilton syringe. The injected dose equivalent was plaque assayed on the same day and contained 15,000 ± 2,000 PFU.

Sixteen-day-old animals were injected intracerebrally, using a 1-μl Hamilton syringe, in the forebrain at the left midpupillary line, 2 mm posterior to the eye at 2-mm depth from the skin perpendicular to the skull surface. Each virus injection contained 1,500 PFU of virus in 200 nl ($n = 7$ each). The intranasal dose given to young postnatal day 16 mice was 10,000 PFU in a total of 50 μl applied to both nostrils. Any mouse showing serious neurological dysfunction was given an anesthetic overdose and was considered to have shown a lethal effect of the virus.

**Cell culture.** U87MG human high-grade glioma cells and 4T1 mouse mammary carcinoma cells were obtained from the ATCC (Manassas, VA). Generation of the rU87 cell line stably transfected with the monomeric red fluorescent protein (pDsRed-monomer-C1 [Invitrogen]) was described elsewhere (22, 40). U118MG, U373, and A172 human glioma cell lines and a 9L rat gliosarcoma cell line were kindly provided by R. Matthews (Yale University). A549 and Calu-1 human lung carcinoma and T-47D and MCF-7 human breast carcinoma cells were supplied by the Yale Cancer Center (Yale University). Primary cultures of adult human brain cells were prepared from human temporal lobectomy material removed for intractable epilepsy solely for the benefit of the patient, and the use was approved by the Yale University Human Investigation Committee. In detail, surgery samples were cut into small cubes, digested with 0.25% trypsin for 15 min, and placed onto Millipore cell culture filter insets over a supply of minimal essential medium (MEM) (Gibco) containing 25% fetal bovine serum (FBS). Five to 7 days later, cells that grew onto the filter membrane from the tissue block were harvested and maintained in MEM supplemented with 10% FBS. Astrocytic lineage was confirmed with immunohistochemistry. The following mouse glioma cell lines were used in the study: CT2A cells (a gift from T. Seyfried, Boston College—Chestnut Hill, Chestnut Hill, MA) and DBT mouse glioma cells (kindly supplied by J. O. Fleming, University of Wisconsin—Madison). The cells were maintained in MEM (Gibco) supplemented with 10% FBS, 1% sodium pyruvate, 100 μM nonessential amino acids, 10 mM HEPES buffer.

**Quantitative real-time PCR.** Brain tissues and cell cultures were lysed, and RNA was extracted using TRIzol reagent (Invitrogen) according to the manufacturer's instructions. Primary cultures of adult human glia cells were grown in 12-well plates and infected with VSV-G/GFP or VSV-CT9-M51 at a multiplicity of infection (MOI) of 2 for 6 h. Triplicate glia cultures infected with each virus and mock-infected cells were lysed, and RNA was extracted. Total RNA was reverse transcribed using the SuperScript III RT kit (Invitrogen) with random hexamers. Quantitative PCR was performed using an IQ iCycler Real-Time PCR Thermocycler (Bio-Rad) and the following TaqMan Gene Expression assays (ABI): human MxA (catalog no. Hs00182073_m1), human ISG15 (catalog no. Hs00192713_m1), and human GAPDH (glyceraldehyde-3-phosphate dehydrogenase) (catalog no. Hs99999905_m1). The following endogenous control assays (ABI) were also used: human ACTB (part no. 4333762E) and mouse ACTB (part no. 4352933E). A custom TaqMan assay with the following specifications was used to detect VSV N/P: forward primer, 5′-CCT AAG AGA GAA GAC AAT TGG CAA GT-3′; reverse primer, 5′-TCC ATG ATA TCT GTT AGT TTT TTT CAT ATG TAG CA-3′; 6-carboxyfluorescein dye probe, 5′-ACA AAT GAC CCT ATA ATT CT-3′. All quantitative PCR was performed using the TaqMan Gene Expression Master Mix (ABI) and a two-step PCR protocol consisting of a hot start at 95°C for 10 min, followed by 40 cycles of 95°C for 15 s and 60°C for 1 min. All results were normalized with respect to beta-actin expression.

**Immunohistochemistry for cellular characterization.** After fixation with paraformaldehyde and permeabilization with 0.2% Triton X-100 of either infected cell cultures or mouse brain infected with virus, mouse antisera against the neuronal antigen Neu N and against the astrocyte marker glial fibrillary acidic protein (GFAP), both from Chemicon, were used at a 1:1,000 dilution for several hours. After multiple washes, a secondary antibody, goat or donkey anti-mouse antibody conjugated to the red fluorophore Alexa 594 (Invitrogen-Molecular Probes, Eugene, OR), was used to immunostain the antigens of interest.

**Immunofluorescence for IRF3.** For interferon regulatory factor 3 (IRF3) and cleaved caspase 3 immunocytochemistry, adult human astrocytes on 6-mm spot slides (Electron Microscopy Sciences, Fort Washington, PA) were fixed in 4% paraformaldehyde and incubated with a 1:100 dilution of polyclonal rabbit anti-IRF3 antiserum (Santa Cruz Biotechnology, Santa Cruz, CA) or a 1:100 dilution of rabbit anti-cleaved caspase antiserum (Cell Signaling, MA), followed by detection with a 1:200 dilution of donkey anti-rabbit immunoglobulin–Alexa Fluor 594.

## RESULTS

Prior to immunization experiments, we first determined the relative toxicities of VSVs within the brain.

**VSV-CT1 and VSV-CT9-M51 result in longer survival after intracerebral injections in young mice.** Introduction of VSV in mice can result in deadly encephalitis, and the severity of the disease and susceptibility of the animals are far greater in newborn and immature mice. We used 16-day-old mice to compare the neurovirulence of the two attenuated VSV mutants to that of VSV-G/GFP. Sixteen-day-old Swiss-Webster mice were injected in the forebrain with the VSV strain being tested. A small injection volume of 200 nl was used. VSV-G/GFP-, VSV-CT1-, and VSV-CT9-M51-injected animals survived an average of 2.7 ± 0.5, 3.3 ± 1.1, and 5.7 ± 0.5 days after intracerebral injection, respectively (Fig. 1A). Survival for VSV-CT9-M51 was significantly longer than for VSV-G/GFP ($P < 0.05$).

**Attenuated VSVs are less neuroinvasive than VSV-G/GFP.** VSV enters the brain by the olfactory nerve after intranasal inoculation. After reaching the olfactory bulb, VSV can spread to and infect distinct periventricular aminergic nuclei, including the locus ceruleus and the raphe (36). After an intranasal inoculation of 10,000 PFU of VSV-G/GFP at postnatal day 16,

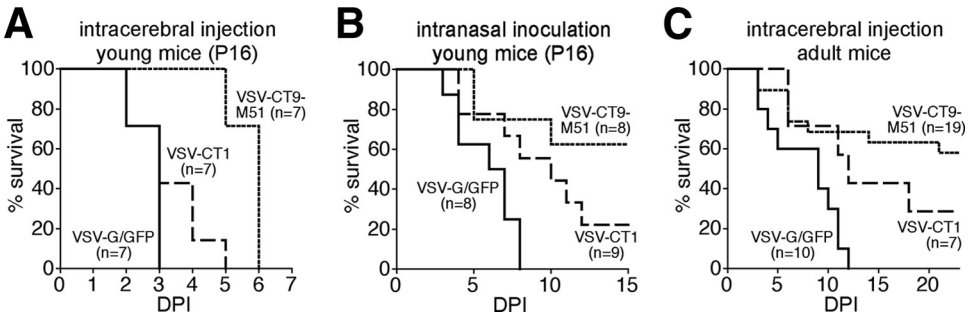


FIG. 1. VSV-CT1 and VSV-CT9-M51 are less neurovirulent and less neuroinvasive. Both attenuated strains and VSV-G/GFP were injected intracerebrally into 16-day-old mice to assess neurovirulence. (A) Young mice are very susceptible to viral encephalitis, and all of the animals died after a forebrain injection of 1,500 PFU. Animals injected with either mutant survived significantly longer than VSV-G/GFP-injected animals. (B) VSV can enter the CNS after intranasal inoculations, but an immune response usually limits or slows down the infection within the olfactory system. To compare the neuroinvasiveness levels of the three strains, 10,000 PFU of either virus was intranasally administered to mice of the same age. All VSV-G/GFP-inoculated animals died, but 22% of VSV-CT1- and 63% of VSV-CT9-M51-injected animals survived. (C) Similarly, after intracerebral injections of 15,000 PFU in less susceptible 5-week-old animals, all animals injected with VSV-G/GFP died. DPI, days postinoculation.

all animals died at a mean of 5.9 ± 2 days. In contrast, five out of eight (62%) VSV-CT9-M51-treated and two out of nine (22%) VSV-CT1-inoculated animals were alive and free of neurological complications 28 days after the intranasal dose. In those VSV-CT1- and VSV-CT9-M51-inoculated animals that succumbed to VSV encephalitis, the mean duration to death was longer than in VSV-G/GFP-treated animals at 8 ± 3.2 days and 6.7 ± 2.9 days, respectively (Fig. 1B).

**Reduced morbidity after intracerebral injection of recombinant VSV.** Stereotactic intracerebral injections of VSV-G/GFP in adult animals resulted in 100% mortality in the injected cohort ($n = 10$). In contrast, partial survival was seen in mice that were injected with the attenuated recombinant VSVs. Eleven out of 19 (58%) mice inoculated with VSV-CT9-M51 survived, with an initial drop in body weight that recovered within a week (see details below). Two out of 7 (29%) mice inoculated with VSV-CT1 survived (Fig. 1C). The mean time to morbidity was delayed with the attenuated mutants at 7.4 ± 2.2 days for VSV-CT9-M51 and 9.6 ± 2.2 days for VSV-CT1 compared to 6.7 ± 1.1 days for VSV-G/GFP-inoculated mice, though this difference did not reach statistical significance ($P = 0.56$; $n = 8$, 5, and 10, respectively; analysis of variance).

To determine the effects of the attenuated phenotype on the extent and pattern of VSV infection in the brain, we analyzed serial brain sections at 1 and 2 days postinoculation for signs of infection at the injection site and at 3 days postinoculation for assessing viral spread. Both VSV-G/GFP and VSV-CT9-M51 expressed the green fluorescent reporter gene in individual infected cells around the injection site (Fig. 2A to D). The placement of the injection and the extent of infection around the injection site were consistent in all animals regardless of the virus used. Marked GFP expression was found at the injection site in all 10 animals. When brains were analyzed at 3 days postinoculation, a commonly infected brain region was the striatum (Fig. 2E and F). Other regions of the brain that showed viral infection included the corpus callosum, septum, cingulate cortex, motor cortex, substantia nigra, and hypothalamus. Infection in the ependyma and periventricular parenchyma was found in the olfactory, lateral, and third ventricles in the VSV-G/GFP-injected animals. In mice that survived intracranial challenge with VSV-CT9-M51, histological analysis at 3 months postinoculation showed no residual viral GFP expression. Clear scar formation at the injection track was noted (Fig. 2G and H) in mice surviving infection.

**Quantitative comparison of viral loads after intracranial injection of VSV variants.** To compare potential differences in replication in the brain, we inoculated similar viral loads intracranially into normal mouse brains ($n = 8$ for VSV-G/GFP; $n = 7$ for VSV-CT9-M51) and harvested the brains 4 days later. To determine virus loads, we quantified viral genomes in whole brains using a sequence that spanned the VSV N and P genes by quantitative PCR. The virus with the greatest replication was VSV-G/GFP, and the virus with the least replication was VSV-CT9-M51 (Fig. 3A). We also compared plaque sizes in vitro for the same two viruses. The plaques and the numbers of dead cells were considerably larger for VSV-G/GFP than for VSV-CT9-M51 (Fig. 3B).

**No differences in the spectra of cellular targets after intracranial injection between VSV variants.** We tested VSV-G/GFP and VSV-CT9-M51 to examine cellular targets in vivo and in vitro. We found no detectable difference in the identities of infected cells, using antisera against Neu N to detect neurons or GFAP to detect astrocytes, between the two viruses (Fig. 3 C-J).

**Intranasal and intramuscular immunizations eliminate VSV-related morbidity and mortality.** VSV induces a very strong adaptive immune response that effectively limits peripheral systemic VSV infections (20). However, little is known about the extent to which a previous peripheral exposure to VSV may impact its neuropathology. Since intracerebral injection of wild-type-based VSV-G/GFP resulted in fatal encephalitis and attenuated variants showed partial mortality, we tested whether immunization could protect mice against intracerebral challenge with VSV. Five-week-old Swiss-Webster mice were divided into one nonimmunized control group and one group that was immunized either intranasally or with an intranasal-intramuscular combination of VSV-G/GFP. The immunized animals received a secondary immunization of VSV after 6 weeks. Two weeks after the secondary immunization, both immunized and nonimmunized mice were challenged with an

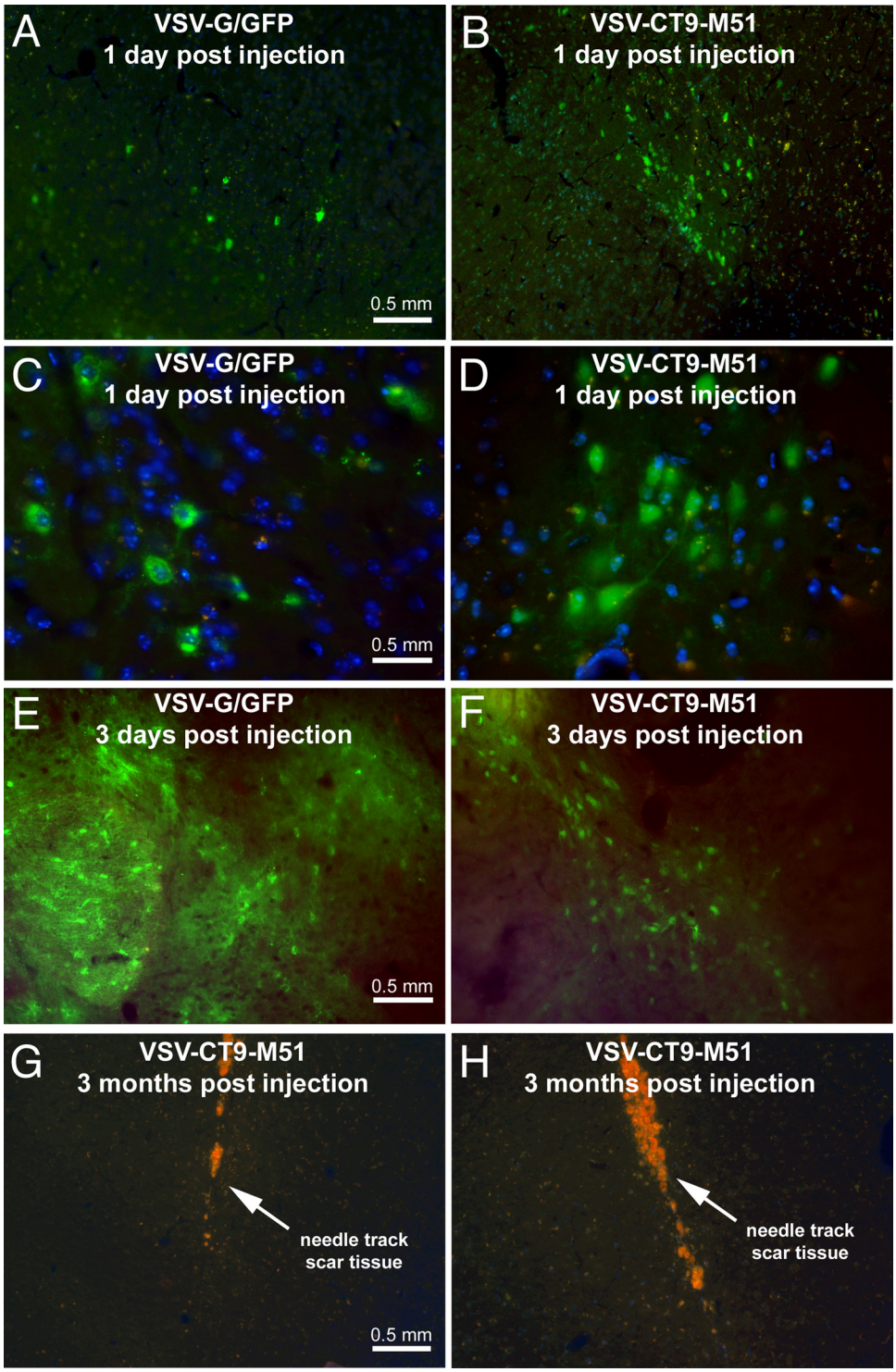


FIG. 2. VSV-G/GFP and VSV-CT9-M51 intracerebral injections result in infection at the injection site and distant sites in the mouse brain. (A and B) Adult Swiss-Webster mice were stereotactically injected in the left frontal lobe with 1,500 PFU of VSV-G/GFP (A) or VSV-CT9-M51 (B). (C and D) One day after the procedure, infected brain cells were encountered at the injection site. DAPI included in the mounting medium was used to visualize cellular nuclei (blue). Infected cells were identified through expression of GFP. (E and F) At 3 days postinoculation, viral spread beyond the injection site was noted. (G and H) Three months after injection, the brains of mice that survived VSV-CT9-M51 challenge showed scar tissue at the area of virus injection. The orange color reflects scar tissue autofluorescence.

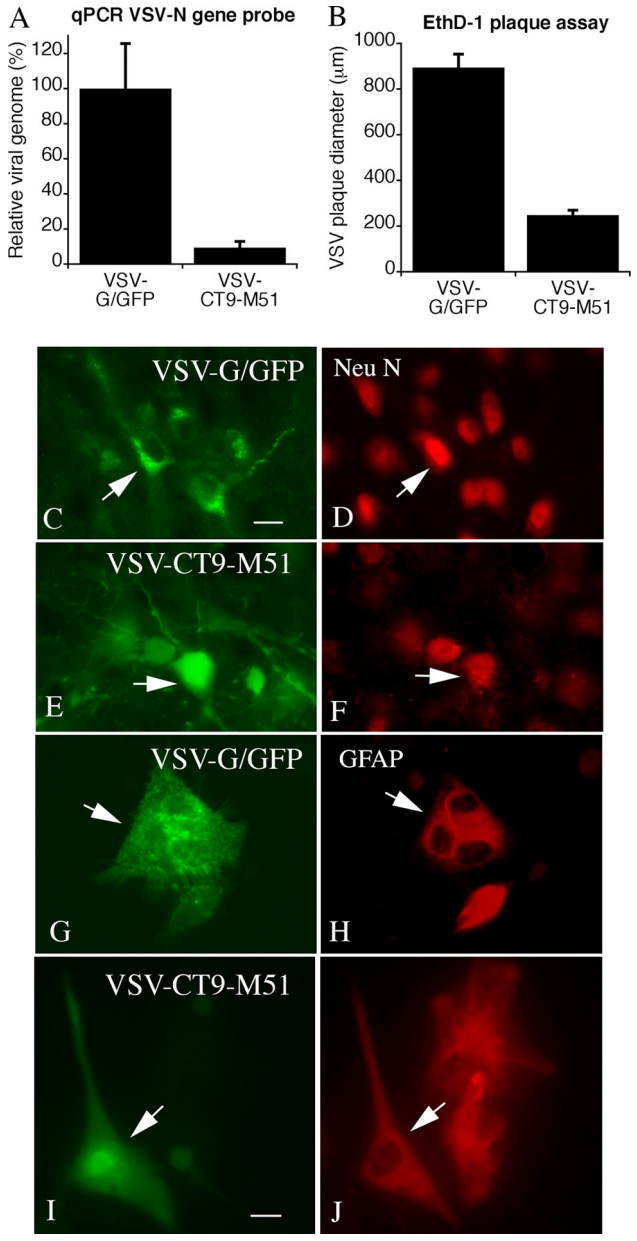


FIG. 3. Viral loads in the brain and cellular targets of VSV-G/GFP and VSV-CT9-M51. The brains of mice injected with equal doses of VSV-G/GFP or VSV-CT9-M51 were harvested 4 days p.i. RNA from homogenized brains was reverse transcribed, and viral titers were assessed using quantitative PCR (qPCR). (A) A PCR probe spanning VSV genes N and P was used to allow detection of genomic VSV copies. Brains infected with VSV-CT9-M51 contained significantly less virus than brains infected with VSV-G/GFP after 4 days. The error bars indicate standard errors of the mean. (B) Cultures of normal mouse brain were infected with 100 PFU of VSV-G/GFP or VSV-CT9-M51 and analyzed 24 h later. Plaques were stained with ethidium homodimer (EthD-1) that stains cells killed by the virus, and the diameters of the plaques were measured. The bar graph shows the relative sizes of the plaques, with VSV-G/GFP generating the largest plaques, indicating a higher rate of infection and replication. (C to J) Viral infections (left) (green, GFP) and immunostaining of the same region (right) (red immunostain). VSV-G/GFP (C, D, G, and H) and VSV-CT9-M51 (E, F, I, and J) were used to infect mouse brains (the mice were euthanized 2 days later) (C to F) or mouse brain cultures (G to J). Red immunostaining for Neu N revealed infections of neurons (D and F), and staining for GFAP (H and J) revealed astrocyte infections. The arrows indicate infected cells that stained for the respective antigen. Scale bars, 12 μm (C through F) and 7 μm (G through J).

intracerebral injection of either VSV-G/GFP ($n = 17$; 7 immunized and 10 nonimmunized), VSV-CT1 ($n = 14$; 7 immunized and 7 nonimmunized), or VSV-CT9-M51 ($n = 32$; 13 immunized and 19 nonimmunized).

A primary result was that all immunized mice ($n = 27$) survived intracerebral injection of VSV. Even mice receiving VSV-G/GFP, a wild-type-based VSV with a GFP reporter, were completely protected when immunized, whereas all nonimmunized control mice receiving intracerebral VSV-G/GFP succumbed to VSV encephalitis (Fig. 4A) after a mean time to lethality of 6.7 ± 1.1 days ($n = 10$). After intracerebral inoculation, immunized mice did not display signs of distress, the fur remained groomed, and any weight change was moderate. In contrast, many of the nonimmunized mice showed severe responses to intracranial VSV inoculation.

Although they were not quantified, we also observed other signs of viral infection, including decreases in motor activity and fur changes, that were not observed in the immunized animals after intracerebral injections. None of the immunized and VSV-challenged animals (VSV-G/GFP, $n = 7$; VSV-CT1, $n = 7$; and VSV-CT9-M51, $n = 13$) developed neurological findings during the 3-month observation period following intracranial injection of the virus. Considering the above-reported neurological morbidity incidence in VSV-CT1-injected and in VSV-CT9-M51-injected nonimmunized animals, the immunization resulted in a significantly reduced incidence ($P = 0.005$; chi-square test) of neurological dysfunction.

After intracerebral injection, immunized and nonimmunized mice showed weight loss (Fig. 4B). The maximum weight losses for immunized animals compared to nonimmunized control mice were 5.7 ± 1.1 g to 30.4 ± 1.3 g for VSV-G/GFP, 7.0 ± 0.7 g to 21.9 ± 4.6 g for VSV-CT1, and 9.1 ± 1.7 g to 13.5 ± 5.3 g for VSV-CT9-M51.

Two routes of immunization were used, intranasal and intramuscular. No difference in animal weight or protective potential was observed between the two paths of immunization, and therefore, the groups were pooled. Following primary immunization, the mice went through a phase of moderate weight loss compared to nonimmunized controls. The weight loss had a rapid onset, starting 1 day after virus inoculation and reaching a maximum of 5.3% ± 0.6% on the second day. The mice started to steadily gain weight after 5 days (Fig. 4C). This temporary weight loss is consistent with previous studies using VSV as a vaccination vector (23, 26). In contrast, the secondary immunization (boost) 6 weeks later did not result in significant weight loss, reflecting systemic protection through the primary immunization (Fig. 4C).

**VSV-CT9-M51 retains oncolytic activity against a wide variety of cancers in vitro.** The experiments described above demonstrate that VSV-CT9-M51 shows the most attenuated neurovirulence of the VSVs compared here and that immunization provides further protection against VSV-CT9-M51 injections into the brain. VSV has been proposed as a potential oncolytic virus that can target various forms of cancer (33). Modifications in the VSV genome that generate attenuated phenotypes may alter the oncolytic potency. To test whether VSV-CT9-M51 retained its oncolytic activity against a wide variety of human cancers, we tested nine different human cancer cell lines, which included four different high-grade gliomas (A172, U87, U118, and U373), two lung cancer cell lines

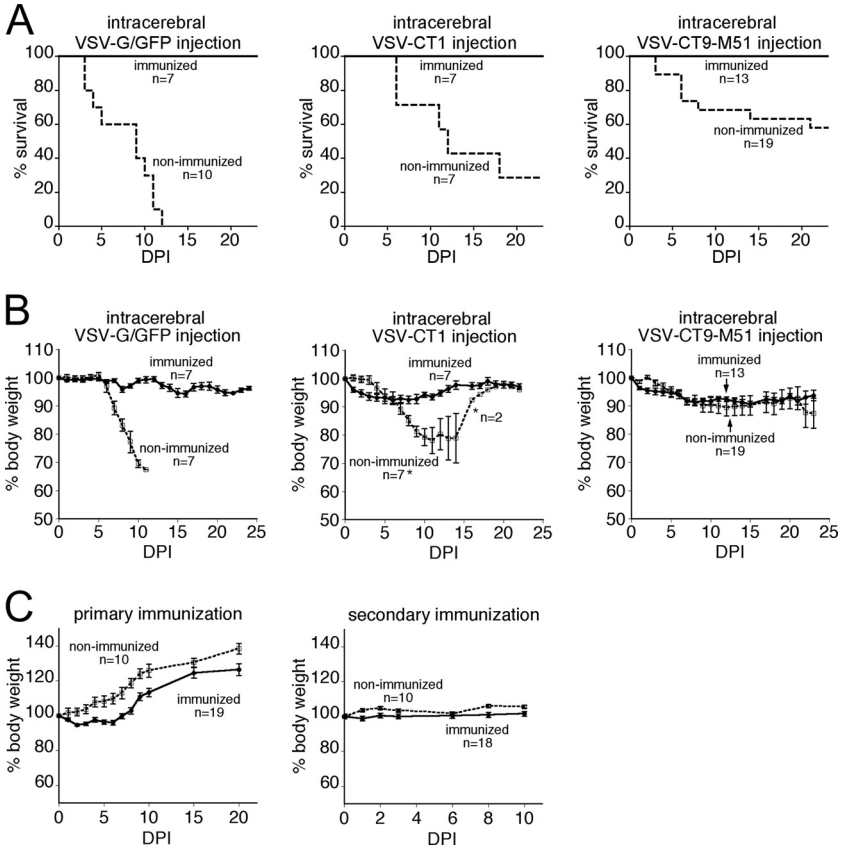


FIG. 4. Peripheral immunization provides complete protection of mice against intracranial challenge with VSV. Five-week-old mice received a primary immunization with a combined intranasal-intramuscular VSV-G/GFP dose followed by a boost 6 weeks later. Two weeks after the VSV boost, the mice were challenged with an intracranial injection of VSV-G/GFP, VSV-CT1, or VSV-CT9-M51. (A) Immunized mice were protected against the lethal effect of intracranial injection of VSV-G/GFP, VSV-CT1, and VSV-CT9-M51. Nonimmunized mice displayed 100% mortality upon VSV-G/GFP infection but showed partial survival with attenuated VSV-CT1 and VSV-CT9-M51. (B) Immunized mice that were protected from virus injection into the brain showed only mild weight loss. (C) Immunized mice experienced transient weight loss after primary, but not secondary, peripheral immunization. The error bars indicate standard errors. DPI, days postinoculation.

(Calu-1 and A-549), and two breast cancer cell lines (T47-D and MCF-7). We included breast and lung cancer cell lines in this battery, since systemic cancers can metastasize to the brain and are in fact more commonly observed than primary brain malignancies. All four glioma cell lines tested were susceptible to complete VSV-mediated cell destruction. An MOI of 1 led to >95% cell death at 24 h postinfection (p.i.) for U118, 36 h p.i. for U87, 48 h p.i. for A-172, and 72 h p.i. for U373 cells. The two lung cancer lines showed >95% cell death at 24 h p.i. (A-549) and 120 h p.i. (Calu-1). The two breast cancer cell lines showed >95% cell death at 36 h p.i. (MCF-7) and 72 h p.i. (T47-D).

Since one of our goals was to improve a potentially therapeutic tool for treating human cancer, we focused on human cancer cell lines. However, due to the possibility of utilizing syngeneic rodent cancer models, we also tested VSV-CT9-M51 on mouse and rat cancer cell lines. After infecting cells at an MOI of 1 with VSV-CT9-M51, >95% cell death was observed at 24 h p.i. for rat 9L gliosarcoma cultures, 36 h p.i. for DBT mouse glioblastoma cells, and 48 h p.i. for CT2A mouse glioma. Together, these data show that despite its attenuated phenotype, VSV-CT9-M51 remains highly oncolytic against a multitude of both human and rodent cancer cell lines.

**Human brain cells mount a robust interferon response to VSV-CT9-M51.** One mechanism that may account for the reduced neurovirulence of VSV-CT9-M51 is a reduced ability of the virus to replicate and to block the intrinisic interferon-inducible gene response of infected cells. The M protein of VSV blocks the transport of cellular mRNAs, including that of the antiviral protein interferon. VSV mutants with an M51 genotype are impaired in the capability to interfere with cellular mRNA transport (33) and therefore may induce a stronger cellular immune response (2). As VSV-CT9-M51 showed reduced neurovirulence compared with VSV-CT1, we focused on VSV-CT9-M51 and its parent virus, VSV-G/GFP. We compared the responses of adult human astrocytes to VSV-G/GFP and VSV-CT9-M51 using quantitative reverse transcription-PCR. Primary cultures were established from human temporal lobectomy material, and immunostaining for GFAP revealed >95% astrocyte origin (Fig. 5H to J). Six hours p.i., we observed a statistically significant increase in the expression of two interferon-induced genes, MxA and ISG15, in all VSV-treated cultures (Fig. 5A and B) ($P < 0.05$; analysis of variance). To support these findings, we did immunostaining for the transcription factor IRF3, which translocates from the cytoplasm to the nucleus during an innate cellular immune re-

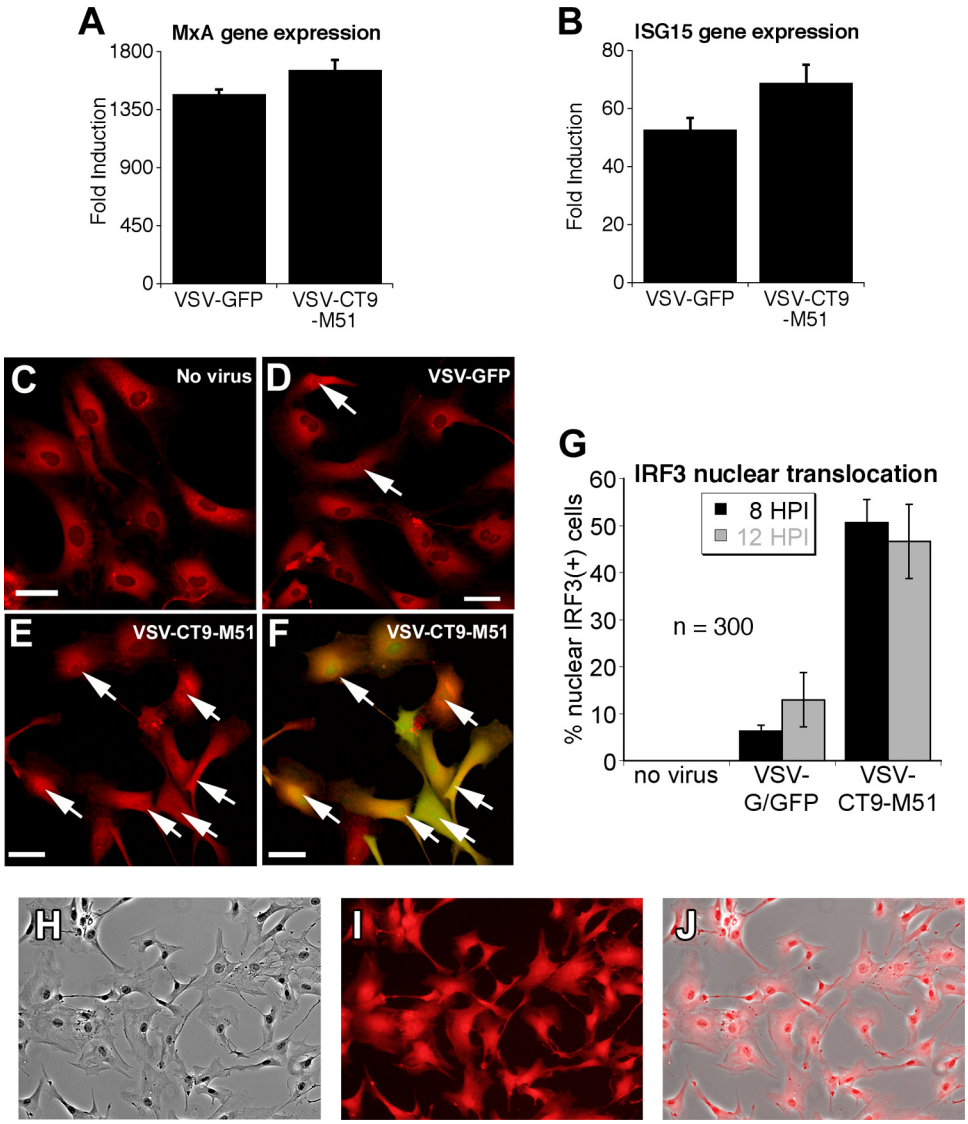


FIG. 5. Human adult astrocytes mount a robust response to VSV-CT9-M51. (A and B) Expression of two downstream interferon genes (ISG15 and MxA) was measured with quantitative reverse transcription-PCR in primary cultures of adult human astrocytes after 6 h of incubation with VSV-G/GFP or VSV-CT9-M51. A more robust induction in interferon-induced gene expression was observed after infection with VSV-CT9-M51 than after infection with VSV-G/GFP. The error bars indicate standard errors. (C to F) Immunofluorescence for the IRF3 transcription factor was used to support the data in panels A and B. IRF3 is a key transcription factor for interferon response that is translocated to the nucleus upon interferon signaling. The arrows mark cells with nuclear labeling of IRF3, indicating nuclear translocation. Significantly more nuclear translocation of IRF3 was demonstrated in adult human astrocytes after VSV-CT9-M51 infection (E) than after VSV-G/GFP infection (D) at two time points (HPI, hours p.i.) after VSV infection (G), which is demonstrated by viral GFP expression (F). Scale bars, 35 μm. (H to J) Immunostaining of cultured cells from adult human brain tissue revealed 100% astrocytic origin. Micrographs are 225 μm wide.

sponse. A greater number of cells showed a nuclear location of IRF3 in response to VSV-CT9-M51 than in response to VSV-GFP (Fig. 5C to F), and the difference was highly significant at 8 and 12 h p.i. ($P < 0.05$; $t$ test) at an MOI of 10 (Fig. 5G). Together, these data suggest that VSV-CT9-M51 may be less invasive in the brain due to the reduced ability of the virus to block intrinsic antiviral defenses.

**Systemic VSV-CT9-M51 targets brain tumors.** In our previous studies, a different virus, VSVrp30, proved capable of targeting and spreading within brain tumors and peripheral glioma grafts and killing tumor cells (22). As described above, VSV-CT9-M51 had attenuated virulence in the brain and was able to efficiently kill glioma cells in vitro. To determine if this attenuated VSV strain would still be able to target glioblastoma in an in vivo intracranial brain tumor model, as a proof of principle, human glioblastoma (U87) cells that expressed a red reporter gene were transplanted into the striata of SCID mice deficient in B and T cells that had not been immunized. Tumors grew with no signs of immune-mediated rejection (Fig. 6A).

Virus was given in the tail vein. VSV-CT9-M51 targeted, infected, spread within, and killed brain tumor xenografts. When we analyzed mice with cerebral tumors at 72 h postinoculation, selective VSV-CT9-M51 infection was found in all

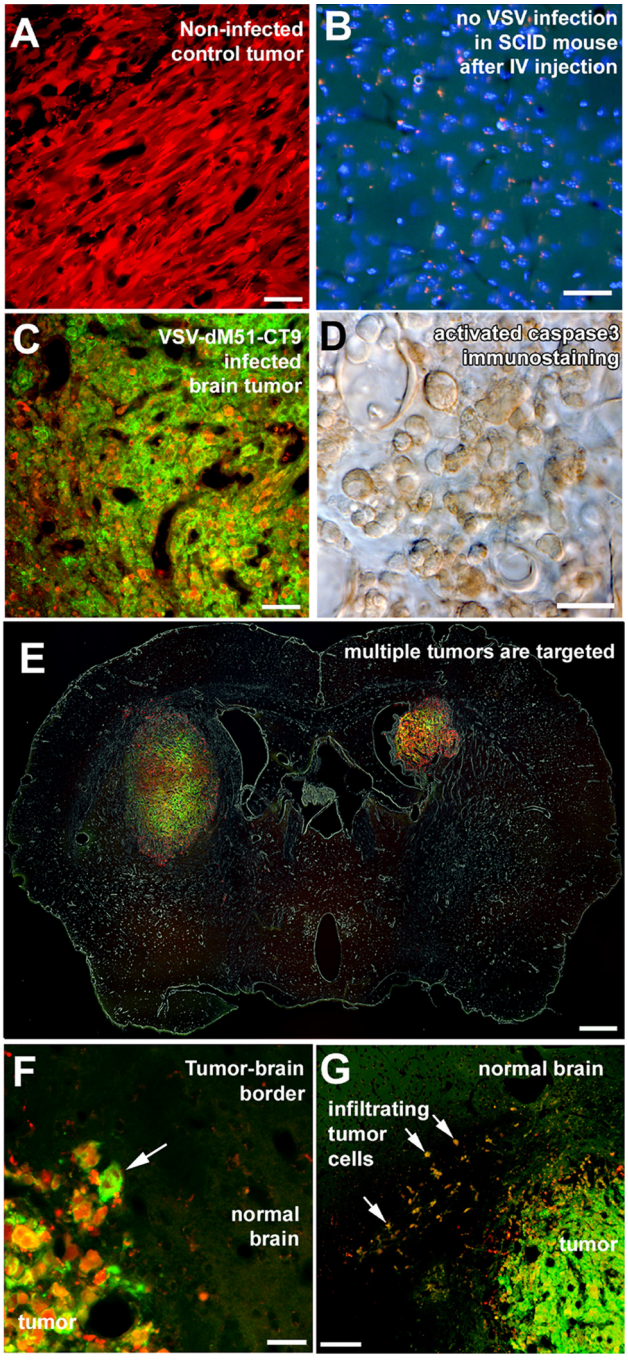


FIG. 6. Neuroattenuated VSV-CT9-M51 targets human glioblastoma transplanted to mouse brains after a single intravenous injection. (A) Human brain tumor cells stably transfected with a red fluorescent protein grew with no signs of spontaneous regression when injected into SCID mouse brains. (B and C) Although an intravenous (IV) injection into control SCID mice did not result in any VSV infection in the brain (B), marked infection was found inside grafted tumors 72 h after intravenous injection of VSV-CT9-M51 (C). (D) Infection of the tumor resulted in widespread apoptosis, as documented by activated caspase 3 immunostaining. (E) Multifocal tumors within the brain were simultaneously infected after intravenous injections. (E and F) Despite robust VSV-CT9-M51 infection inside the tumor (arrow in panel F), no infection was observed outside the tumor anywhere in the mouse brain. (G) Tumor cells that grew infiltratively (arrows), away from the main tumor bulk into the normal brain parenchyma, were also infected, along with the main tumor. Scale bars, 50 μm (A to C), 20 μm (D), 500 μm (E), 25 μm (F), and 300 μm (G).

six (100%) striatal rU87 glioma xenografts in three animals (Fig. 6C). Apoptotic cell death in the infected tumor cells was documented using immunohistochemistry with an antibody recognizing cleaved caspase 3, a late effector of apoptosis. A mean of 97.9% ± 2.6% of the cells stained positively for the antibody (Fig. 6D). The infection within the tumor was highly specific for the tumor cells. Single red fluorescent tumor cells outside the main tumor bulk and infiltrating the normal brain parenchyma were found to be infected with VSV-CT9-M51 without infection of the surrounding normal brain parenchyma (Fig. 6F and G). We also did control experiments to test if VSV-CT9-M51 entered the normal brain (not bearing a tumor) upon systemic injection of the virus. Seventy-two hours after intravenous injection of $10^7$ PFU in SCID mice, no infected cells were found in consecutive serial brain sections (Fig. 6B), indicating that the virus selectively infected the tumor.

## DISCUSSION

Here, we tested the hypothesis that peripheral activation of the systemic immune system can protect the brain from VSV damage. We found that peripheral inoculation with VSV blocked the lethal consequences of VSV injected directly into the brain and provided complete protection from both attenuated recombinant VSVs and nonattenuated VSV. Immunization also prevented the neurological dysfunction associated with CNS infections with VSV. We are unaware of other reports demonstrating the protective effect of peripheral immunization against VSV neurovirulence within the brain.

**Vaccination blocks lethal VSV encephalitis.** When directly injected into the mouse brain, VSV can cause neurological dysfunction or lethal encephalitis (19, 36). The replication cycle of VSV occurs in 3 to 6 h (20), and the rapid generation of viral progeny contributes to the quick spread of VSV in the brain. Outside the brain, VSV is effectively controlled and eliminated by both the innate and systemic branches of the immune system. Peripheral VSV exposure generates a strong B- and T-cell response that effectively controls peripheral rechallenges of the same virus. However, the extent to which a peripheral immunization can provide protection from intracranial VSV challenge has remained unknown. We found that peripheral immunization was protective under all tested conditions. Different routes of peripheral immunization, including intranasal or intramuscular, led to the same level of protection from intracranial VSV challenge. In addition, neuroprotection through peripheral immunization was effective for intracranial challenges with both attenuated VSV strains, VSV-CT1 and VSV-CT9-M51, and the wild-type-based VSV-G/GFP. Direct intracranial VSV injection has been proposed as a more sensitive indicator of neurotoxicity than intranasal virus application (7). Hence, our data suggest that the immune system, once primed against VSV, is effective in controlling and eliminating intracranial VSV spread and neurotoxicity.

**Reduced neurovirulence of attenuated VSV mutants.** A number of VSV mutants have been described (7, 11, 15, 32, 33). Attenuation of the VSV phenotype here was done by using either a virus with the cytoplasmic portion of the G protein truncated from 29 amino acids to a single amino acid (VSV-CT1) or by combining an M51 deletion with a partially trun-

cated G protein reduced to 9 cytoplasmic amino acids. Both of these recombinant VSVs have previously been reported to show an attenuated phenotype after peripheral administration (2, 23, 33). Here, we showed that these recombinant viruses, particularly VSV-CT9-M51, also show reduced neurovirulence within the brain. In all in vivo tests, VSV-CT1 showed a greater degree of neurovirulence than VSV-CT9-M51.

**Attenuated VSV targets brain cancer.** VSV has gained attention as a promising biological anticancer agent against a variety of malignancies. Malignant brain tumors have been successfully targeted by VSV in laboratory studies (18, 22), but virus spread through the CNS and neurotoxicity remain challenges to be addressed. Previous work showed that an M51 mutant VSV was able to target brain tumors (18). As further molecular attenuation might reduce the oncolytic targeting of VSV, we tested whether the doubly attenuated virus can target cancer cells in vivo. We showed that VSV-CT9-M51, even with two attenuating mutations involving M51 and a reduction in the length of the cytoplasmic tail of the G protein, is still able to target selectively, spread within, and kill human glioblastoma after intravenous inoculation. This dual-recombinant VSV not only can target brain tumors, but also shows reduced intrinsic neurovirulence upon injection into the brain and after intranasal application and can be further controlled by peripheral immunization.

**Increased ISG15 and MxA induction by VSV-CT9-M51.** The crucial role of intrinsic immunity is illustrated by mice lacking interferon receptors that showed enhanced mortality upon VSV infection despite having an intact systemic immune system (21). Interferon-inducible genes play an essential role in defending the brain from VSV infection (35, 40). In all three experiments comparing the neurovirulence levels of the three VSVs used here, VSV-CT9-M51 was the least neurovirulent. We tested the hypothesis that this may be due in part to a shift in the ability of the intrinsic immune system to block viral infections. We found that the interferon-inducible downstream ISG15 and MxA genes were upregulated to a greater extent in control adult human astrocytes by VSV-CT9-M51 than by the other tested strains of VSV. Similarly, VSV-CT9-M51 induced more nuclear translocation of IRF3 than did VSV-G/GFP. As controls for human tumor cells, we used primary cultures from human epileptic foci. Although possibly not normal, these cells are nonmalignant and nontransformed in nature and hence may serve as controls for cancer cells. Finally, VSV-CT9-M51 showed reduced replication in vivo and reduced plaque size and cell death on normal brain cells in vitro compared with VSV-G/GFP.

In summary, we showed that immunization protects the brain from intracerebral injection of all of the VSV variants tested. In the absence of immunization, of the three VSVs examined here, VSV-CT9-M51 was the most attenuated in terms of brain infection in both immature and mature hosts.

## ACKNOWLEDGMENTS

We thank J. Rose for suggestions and for recombinant VSVs, V. Rogulin and Y. Yang for excellent technical facilitation, and J. M. Piepmeier and D. D. Spencer for tissue and suggestions.

Support was provided by NIH grants A1/NS48854 and CA124737 to A.N.V.D.P.

## REFERENCES

1. **Ahmed, M., S. D. Cramer, and D. S. Lyles.** 2004. Sensitivity of prostate tumors to wild type and M protein mutant vesicular stomatitis viruses. Virology **330:**34–49.
2. **Ahmed, M., T. R. Marino, S. Puckett, N. D. Kock, and D. S. Lyles.** 2008. Immune response in the absence of neurovirulence in mice infected with M protein mutant vesicular stomatitis virus. J. Virol. **82:**9273–9277.
3. **Balachandran, S., M. Porosnicu, and G. N. Barber.** 2001. Oncolytic activity of vesicular stomatitis virus is effective against tumors exhibiting aberrant p53, Ras, or myc function and involves the induction of apoptosis. J. Virol. **75:**3474–3479.
4. **Baldridge, J. R., B. D. Pearce, B. S. Parekh, and M. J. Buchmeier.** 1993. Teratogenic effects of neonatal arenavirus infection on the developing rat cerebellum are abrogated by passive immunotherapy. Virology **197:**669–677.
5. **Bi, Z., M. Barna, T. Komatsu, and C. S. Reiss.** 1995. Vesicular stomatitis virus infection of the central nervous system activates both innate and acquired immunity. J. Virol. **69:**6466–6472.
6. **Christian, A. Y., M. Barna, Z. Bi, and C. S. Reiss.** 1996. Host immune response to vesicular stomatitis virus infection of the central nervous system in C57BL/6 mice. Viral Immunol. **9:**195–205.
7. **Clarke, D. K., F. Nasar, M. Lee, J. E. Johnson, K. Wright, P. Calderon, M. Guo, R. Natuk, D. Cooper, R. M. Hendry, and S. A. Udem.** 2007. Synergistic attenuation of vesicular stomatitis virus by combination of specific G gene truncations and N gene translocations. J. Virol. **81:**2056–2064.
8. **Dalton, K. P., and J. K. Rose.** 2001. Vesicular stomatitis virus glycoprotein containing the entire green fluorescent protein on its cytoplasmic domain is incorporated efficiently into virus particles. Virology **279:**414–421.
9. **Duntsch, C. D., Q. Zhou, H. R. Jayakar, J. D. Weimar, J. H. Robertson, L. M. Pfeffer, L. Wang, Z. Xiang, and M. A. Whitt.** 2004. Recombinant vesicular stomatitis virus vectors as oncolytic agents in the treatment of high-grade gliomas in an organotypic brain tissue slice-glioma coculture model. J. Neurosurg. **100:**1049–1059.
10. **Ebert, O., S. Harbaran, K. Shinozaki, and S. L. Woo.** 2005. Systemic therapy of experimental breast cancer metastases by mutant vesicular stomatitis virus in immune-competent mice. Cancer Gene Ther. **12:**350–358.
11. **Flanagan, E. B., T. R. Schoeb, and G. W. Wertz.** 2003. Vesicular stomatitis viruses with rearranged genomes have altered invasiveness and neuropathogenesis in mice. J. Virol. **77:**5740–5748.
12. **Gearhart, M. A., P. A. Webb, A. P. Knight, M. D. Salman, J. A. Smith, and G. A. Erickson.** 1987. Serum neutralizing antibody titers in dairy cattle administered an inactivated vesicular stomatitis virus vaccine. J. Am. Vet. Med. Assoc. **191:**819–822.
13. **Gobet, R., A. Cerny, E. Rüedi, H. Hengartner, and R. M. Zinkernagel.** 1988. The role of antibodies in natural and acquired resistance of mice to vesicular stomatitis virus. Exp. Cell Biol. **56:**175–180.
14. **Jackson, A. C.** 2008. Rabies. Neurol. Clin. **26:**717–726.
15. **Johnson, J. E., F. Nasar, J. W. Coleman, R. E. Price, A. Javadian, K. Draper, M. Lee, P. A. Reilly, D. K. Clarke, R. M. Hendry, and S. A. Udem.** 2007. Neurovirulence properties of recombinant vesicular stomatitis virus vectors in non-human primates. Virology **360:**36–49.
16. **Jones, S. M., H. Feldmann, U. Ströher, J. B. Geisbert, L. Fernando, A. Grolla, H. D. Klenk, N. J. Sullivan, V. E. Volchkov, E. A. Fritz, K. M. Daddario, L. E. Hensley, P. B. Jahrling, and T. W. Geisbert.** 2005. Live attenuated recombinant vaccine protects nonhuman primates against Ebola and Marburg viruses. Nat. Med. **11:**786–790.
17. **Lawson, N. D., E. A. Stillman, M. A. Whitt, and J. K. Rose.** 1995. Recombinant vesicular stomatitis viruses from DNA. Proc. Natl. Acad. Sci. USA **92:**4477–4481.
18. **Lun, X., D. L. Senger, T. Alain, A. Oprea, K. Parato, D. Stojdl, B. Lichty, A. Power, R. N. Johnston, M. Hamilton, I. Parney, J. C. Bell, and P. A. Forsyth.** 2006. Effects of intravenously administered recombinant vesicular stomatitis virus ($VSV_{\Delta M51}$) on multifocal and invasive gliomas. J. Natl. Cancer Inst. **98:**1546–1557.
19. **Lundh, B., A. Löve, K. Kristensson, and E. Norrby.** 1988. Non-lethal infection of aminergic reticular core neurons: age-dependent spread of ts mutant vesicular stomatitis virus from the nose. J. Neuropathol. Exp. Neurol. **47:**497–506.
20. **Lyles, D. S., and C. E. Rupprecht.** 2007. Rhabdoviridae, p. 1363–1408. *In* D. M. Knipe and P. M. Howley (ed.), Fields Virology, 5th ed. Lippincott Williams and Wilkins, Philadelphia, PA.
21. **Müller, U., U. Steinhoff, L. F. Reis, S. Hemmi, J. Pavlovic, R. M. Zinkernagel, and M. Aguet.** 1994. Functional role of type I and type II interferons in antiviral defense. Science **264:**1918–1921.
22. **Ozduman, K., G. Wollmann, J. M. Piepmeier, and A. N. van den Pol.** 2008. Systemic vesicular stomatitis virus selectively destroys multifocal glioma and metastatic carcinoma in brain. J. Neurosci. **28:**1882–1893.
23. **Publicover, J., E. Ramsburg, M. Robek, and J. K. Rose.** 2006. Rapid pathogenesis induced by a vesicular stomatitis virus matrix protein mutant: viral pathogenesis is linked to induction of tumor necrosis factor alpha. J. Virol. **80:**7028–7036.
24. **Reiss, C. S., I. V. Plakhov, and T. Komatsu.** 1998. Viral replication in

olfactory receptor neurons and entry into the olfactory bulb and brain. Ann. N. Y. Acad. Sci. **855:**751–761.

25. **Reuter, J. D., D. L. Gomez, J. H. Wilson, and A. N. van den Pol.** 2004. Systemic immune deficiency necessary for cytomegalovirus invasion of the mature brain. J. Virol. **78:**1473–1487.
26. **Roberts, A., L. Buonocore, R. Price, J. Forman, and J. K. Rose.** 1999. Attenuated vesicular stomatitis viruses as vaccine vectors. J. Virol. **73:**3723–3732.
27. **Rose, N. F., P. A. Marx, A. Luckay, D. F. Nixon, W. J. Moretto, S. M. Donahoe, D. Montefiori, A. Roberts, L. Buonocore, and J. K. Rose.** 2001. An effective AIDS vaccine based on live attenuated vesicular stomatitis virus recombinants. Cell **106:**539–549.
28. **Sabin, A. B., and P. K. Olitsky.** 1937. Influence of host factors on neuroinvasiveness of vesicular stomatitis virus. J. Exp. Med. **66:**15–34.
29. **Saha, K., D. Hollowell, and P. K. Wong.** 1994. Mother-to-baby transfer of humoral immunity against retrovirus-induced neurologic disorders and immunodeficiency. Virology **198:**129–137.
30. **Schneider-Schaulies, J., S. Niewiesk, S. Schneider-Schaulies, and V. ter Meulen.** 1999. Measles virus in the CNS: the role of viral and host factors for the establishment and maintenance of a persistent infection. J. Neurovirol. **5:**613–622.
31. **Schnell, M. J., L. Buonocore, E. Boritz, H. P. Ghosh, R. Chernish, and J. K. Rose.** 1998. Requirement for a non-specific glycoprotein cytoplasmic domain sequence to drive efficient budding of vesicular stomatitis virus. EMBO J. **17:**1289–1296.
32. **Simon, I. D., J. Publicover, and J. K. Rose.** 2007. Replication and propagation of attenuated vesicular stomatitis virus vectors in vivo: vector spread correlates with induction of immune responses and persistence of genomic RNA. J. Virol. **81:**2078–2082.
33. **Stojdl, D. F., B. D. Lichty, B. R. ten Oever, J. M. Paterson, A. T. Power, S. Knowles, R. Marius, J. Reynard, L. Poliquin, H. Atkins, E. G. Brown, R. K. Durbin, J. E. Durbin, J. Hiscott, and J. C. Bell.** 2003. VSV strains with defects in their ability to shutdown innate immunity are potent systemic anti-cancer agents. Cancer Cell **4:**263–275.
34. **Studahl, M.** 2003. Influenza virus and CNS manifestations. J. Clin. Virol. **28:**225–232.
35. **Trottier., M. D., Jr., B. M. Palian, and C. Shoshkes Reiss.** 2005. VSV replication in neurons is inhibited by type I IFN at multiple stages of infection. Virology **333:**215–225.
36. **van den Pol, A. N., K. P. Dalton, and J. K. Rose.** 2002. Relative neurotropism of a recombinant rhabdovirus expressing a green fluorescent envelope glycoprotein. J. Virol. **76:**1309–1327.
37. **van den Pol, A. N., K. Ozduman, G. Wollmann, W. Ho, I. Simon, Y. Yao, J. K. Rose, and P. K. Gosh.** 2009. Viral strategies to study the brain, including a replication-restricted self-amplifying delta-G vesicular stomatitis virus that rapidly expresses transgenes in brain and can generate a multicolor Golgi-like expression. J. Comp. Neurol. **516:**456–481.
38. **Wege, H., R. Watanabe, M. Koga, and Y. Ter Meulen.** 1983. Coronavirus JHM-induced demyelinating encephalomyelitis in rats: influence of immunity on the course of disease. Prog. Brain. Res. **59:**221–231.
39. **Wollmann, G., P. Tattersall, and A. N. van den Pol.** 2005. Targeting human glioblastoma cells: comparison of nine viruses with oncolytic potential. J. Virol. **79:**6005–6022.
40. **Wollmann, G., M. D. Robek, and A. N. van den Pol.** 2007. Variable deficiencies in the interferon response enhance susceptibility to vesicular stomatitis virus oncolytic actions in glioblastoma cells but not in normal human glial cells. J. Virol. **81:**1479–1491.